

A Gamma Ray Observatory  
Ground Attitude Error Analysis Study Using  
The Generalized Calibration System

*E. Ketchum*  
*Code 554/ Flight Dynamics Analysis Branch*  
*Goddard Space Flight Center*  
*Greenbelt, MD 20771*

**ABSTRACT**

The Goddard Space Flight Center (GSFC) Flight Dynamics Division (FDD) will be responsible for performing ground attitude determination for Gamma Ray Observatory (GRO) support. The study reported in this paper provides the FDD and the GRO project with ground attitude determination error information and illustrates several uses of the Generalized Calibration System (GCS). GCS, an institutional software tool in the FDD, automates the computation of the expected attitude determination uncertainty that a spacecraft will encounter during its mission. The GRO project is particularly interested in the uncertainty in the attitude determination using Sun sensors and a magnetometer when both star trackers are inoperable. In order to examine the expected attitude errors for GRO, a systematic approach was developed including various parametric studies. The approach identifies pertinent parameters and combines them to form a matrix of test runs in GCS. This matrix formed the basis for this study.

PRECEDING PAGE BLANK NOT FILMED

## I : INTRODUCTION

The Gamma Ray Observatory (GRO) is a 16,000 Kg scientific satellite that will be launched in the early part of 1990. The GRO, built by TRW, will study gamma ray sources throughout the universe. It will point inertially and fly in a circular orbit 400-450 KM from the Earth's surface. The GRO's onboard attitude sensors include two Fixed Head Star Trackers (FHST's), the NASA standard Inertial Reference Unit (DRIRU-II), an Fine Sun Sensor Assembly (FSSA), a Coarse Sun Sensor Assembly (CSSA), and a Three-Axis Magnetometer (TAM). The focus of this study will be on the FHST's, the Sun sensors, and the TAM.

This study investigates the attitude determination errors, compared to available mission requirements, that are likely to occur during the GRO mission. The various sensor combinations examined included two FHST's, a FSS and a FHST, FSSa (and TAM), and CSS (and TAM). Requirements do not exist for the contingency case involving Sun sensors and magnetometer; the study is interested in just how well the Flight Dynamics Division (FDD) can determine GRO's attitude under these circumstances. The FSS/FHST and FHST/FHST cases three sigma requirements are, respectively, 167.5 arcsec and 86.4 arcsec. This study used the Generalized Calibration System (GCS) to examine the scenarios in light of several geometrical and statistical considerations. GCS, an FDD software tool, was a well suited tool for this project because of its ability to produce large quantities of numerical data. Each sensor set up was also investigated using hand calculations (the TRIAD algorithm), which provided intuitive insight not directly seen in the numerical GCS results. These results were also compared to available mission attitude determination requirements and pre-determined capabilities.

GCS is a software tool that can predict state attitude uncertainties using a batch least squares estimator over a specified data span. GCS is generic and can be adapted to virtually any three axis stabilized or spinning spacecraft. It can model the necessary GRO attitude sensors considered in this study (FSS, CSS, TAM, and FHST). GCS is also able to solve for as well as "consider" parameters such as sensor alignment, bias, and scale factors. For a more detailed discussion of the mathematics that GCS employs, see the appendix and reference 1.

Analysis identified pertinent parameters which addressed the necessary geometric and statistical considerations of the GRO mission. Combining these parameters created a systematic GCS run work matrix. The identified parameters, considered over various sensor combinations, include: time from ascending node (spacecraft position in orbit), time of year (Sun position), data batch size (number of frames considered), as well as sensor misalignment. This study varied the time from ascending node in thirds of an orbit (smaller amounts where interesting) and time of year bi-monthly (and semi-monthly where necessary). A batch consists of one or more "frames", where a frame is a set of measurements all taken at one time. A batch size therefore represents the number of frames taken together with, in this case, approximately one minute intervals between frames. The batch

	FSS/TAM	CSS/TAM	FHST cases
STATISTICAL	batch size: single frame two frames : : 2/3 orbit	batch size: single frame two frames : : 2/3 orbit	batch size: single frame two frames : : 2/3 orbit
GEOMETRY A	s/c position time in orbit: minute intervals around orbit	s/c position time in orbit: minute intervals around orbit	
GEOMETRY B	Sun position time of year:  bi-monthly	Sun position time of year:  bi-monthly	
ALIGNMENT	For FSS/TAM  0 misalignment 1/2 of alignment accuracy spec full spec	for CSS/TAM  0 misalignment 1/2 of spec full spec	for 1)FHST/FSS 2)2 FHSTs 0 misalignment 1/2 of spec full spec

FIGURE 1: WORK MATRIX

size began with single frame solutions and increased in small amounts up to the point where the error is within the requirement (or within reason where no requirement is available). Sensor misalignments were varied from 0 to just over the sensor specification. This information established a GCS work matrix (fig 1); the corresponding GCS runs (using the work matrix as a guideline) identified if and when, with respect to the above parameters, the spacecraft could keep to the attitude determination requirements.

Simple hand calculations using the TRIAD algorithm (ref 2) performed on each sensor combination scenario provided a comparison with and check against the results from GCS. Certain results from the GCS runs can be explained and trusted in light of the hand computations.

The main objective of this project centers on the GRO expected ground attitude determination errors assuming both star trackers are malfunctioning, therefore assuming a sun/magnetometer solution. For comparison and an overall view, nominal scenarios (incorporating the FHST) are also investigated. Results from this study are presented below, contingency cases first followed by the nominal cases. The results are discussed in light of the GCS findings along with hand calculations using the TRIAD algorithm.

## II: Attitude Determination Using Fine Sun Sensor and Magnetometer

### 2.1: Fine Sun Sensor/Magnetometer Configuration

All cases use a 3-2-1 Euler rotation sequence to define the spacecraft attitude. During normal operations, GRO employs at least one FHST for attitude determination. Since the FSS/TAM case is a contingency case, a strictly Sun pointing attitude was assumed which is the nominal backup control mode. Setting up the necessary sensors for the GCS study required modeling GRO's two Fine Sun Sensors as two GCS "Coarse Sun Sensors" (see the appendix), and modeling a TAM. The GCS CSS assumes the boresight to be along the sensor X axis. In order to give the appropriate alignment for GRO's sensors, the three alignment Euler angles (aligning the sensors relative to the spacecraft) used for the two Sun sensors and the TAM are, in degrees (Z,Y,X):

CSS1: (0, -60, 0)

CSS2: (0, 2, 0)

TAM: (180, 0, 0)

Note that in Sun pointing mode, the Sun is only visible to CSS2. Since this sensor points roughly in the +X (roll) direction, it provides primarily pitch and yaw information and poor roll information.

The scale factors and bias for the Sun sensor measurements are assumed to be 1 and 0 respectively as this study expects these calibration constants to be known. The sensor alignment uncertainty is however considered later. Similarly, the TAM bias vector is also assumed to be 0, initially.

The observation uncertainty for the Sun sensors is 0.022 degrees (ref 3 and 4). This study used 0.4 milligauss as the observation uncertainty for the TAM (ref 3 and 4). These values represent one sigma uncertainty.

Following the work matrix described above, the GRO attitude uncertainties were examined in light of several parameters; considering Sun position, spacecraft position in orbit, batch size, and sensor alignment uncertainty.

#### Case 1: Variation of Attitude Uncertainty with Batch Size

This case considers several positions in orbit and times of year as the batch size varies. Varying the uncertainty over batch size for different positions in orbit showed that the uncertainty in the attitude estimation rapidly became uniform in pitch and yaw, and wavered only slightly in roll (fig 3). The only exception occurs during Sun sensor occultation, which appears at a different place in each run. During this occultation, the pitch and yaw solution does not improve, therefore creating a flat area in the graph which consequently moves with the time of the occultation. The single frame uncertainties in pitch and yaw are roughly equal to the uncertainty in the Sun sensor. This is not surprising since these sensors have a higher degree of accuracy than the magnetometer and work to determine the attitude in these directions.

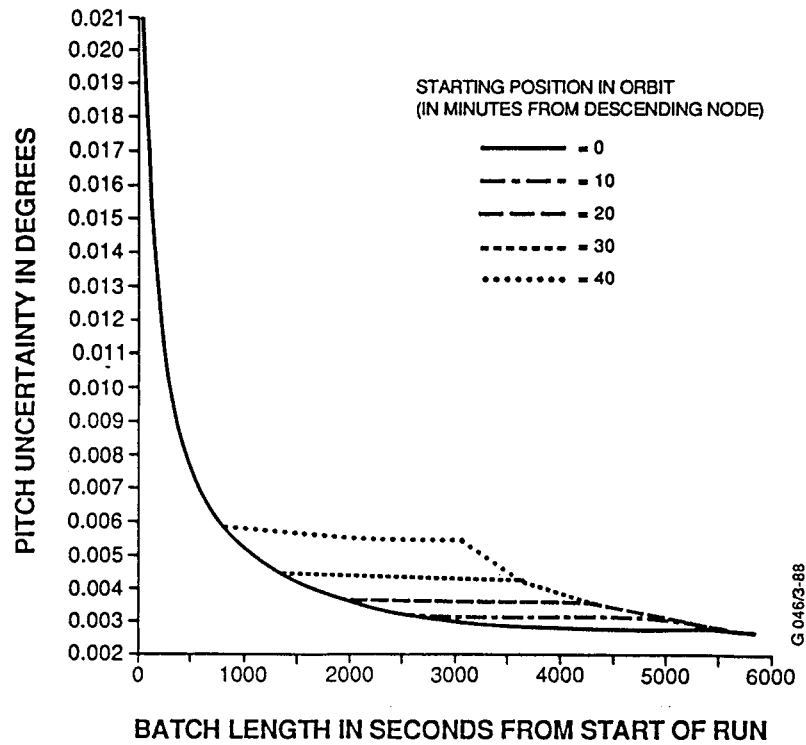


FIGURE 3a  
PITCH UNCERTAINTY vs BATCH LENGTH

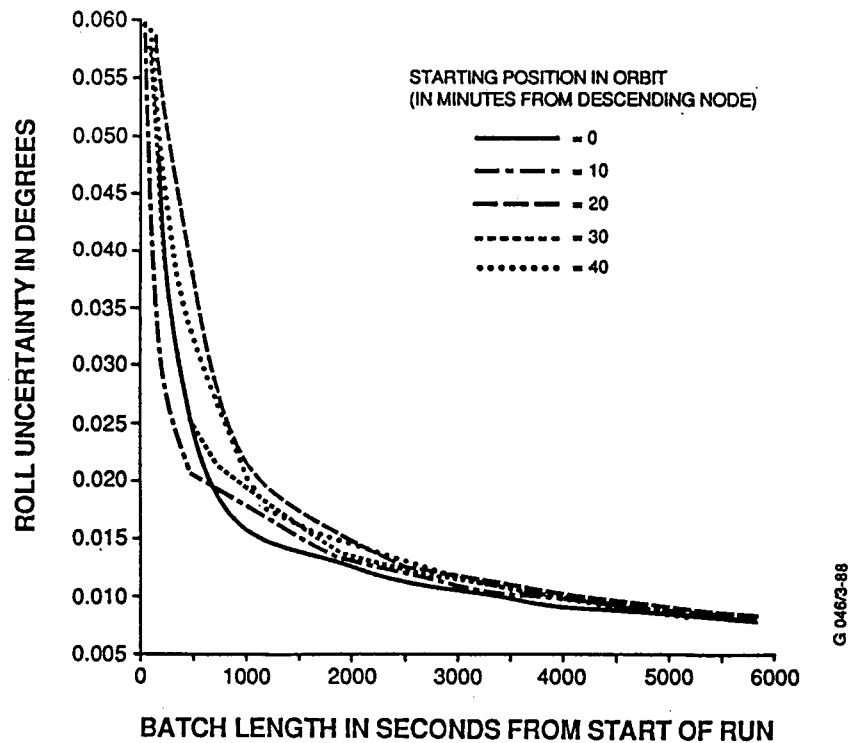


FIGURE 3b  
ROLL UNCERTAINTY vs BATCH LENGTH

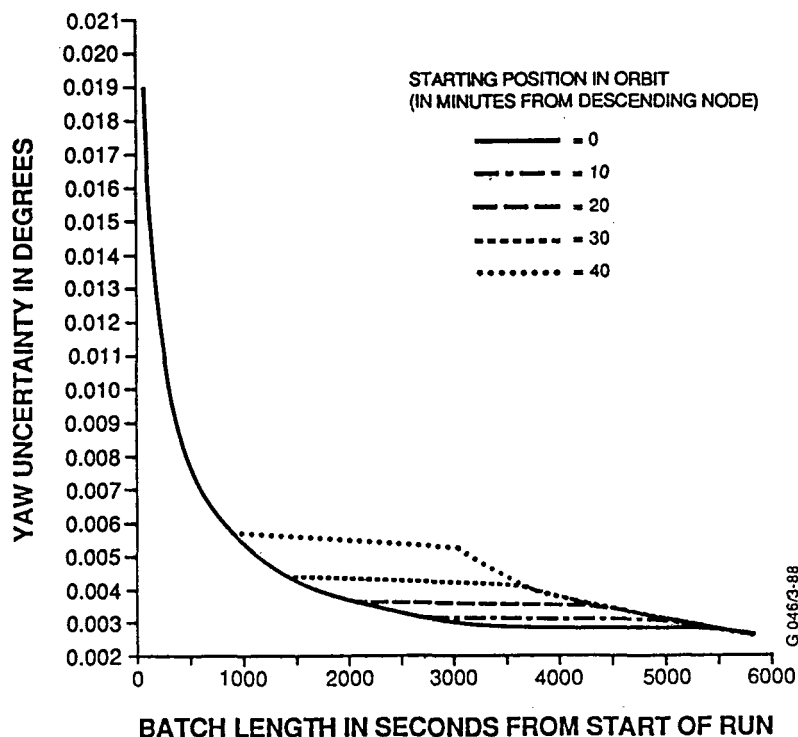


FIGURE 3c  
YAW UNCERTAINTY vs BATCH LENGTH

Unfortunately, these results take into account only the random errors for the magnetometer but neglect systematic errors, particularly in the accuracy in the knowledge of the reference magnetic field. Using results obtained for the change in the magnetic field from 1965 to 1975 (ref 5), and considering that the magnetic field is well determined for 1980, (ref 5), the uncertainty of the field for 1990 can be inferred (ref 5). At the GRO altitude of 450 Km, this uncertainty has a one sigma value of 1.8 milligauss.

The incorporation of the additional magnetic field uncertainty requires careful consideration. Including the uncertainty simply as a bias consider parameter, and leaving the TAM measurement uncertainty unchanged is not satisfactory. GCS assumes that the influence of a measurement estimate is weighted inversely to the measurement's uncertainty (see appendix ), creating adverse results in pitch and yaw. Maintaining the measurement uncertainty of 0.4 milligauss for the TAM means that these measurements are weighted almost half as heavily as the FSS information. As the batch gets bigger and bigger (more and more measurements included) the solution does not improve as it should but instead gets much worse in parts. Yet, in these directions attitude should be well defined in areas where Sun data is

available. The deterioration of the solution exists simply because of the heavy weighting of the increasing amount of poor TAM data.

In the operational attitude determination system, measurement weighting may be specified independently of the true measurement uncertainty. To simulate this in GCS, the TAM measurement uncertainty can be adjusted to include the magnetic field uncertainty. The root-sum-square of the nominal uncertainty of 0.4 milligauss and the additional uncertainty of 1.8 milligauss produces an effective uncertainty of 1.84 milligauss. This results in the proper measurement weighting, but causes GCS to overestimate the intrinsic measurement uncertainty.

The adjusted TAM uncertainty exhibits good results in pitch and yaw (fig 4a and 4c). Note that during Sun occultation, when there is no Sun vector measurement, the poor magnetometer data does cause the solution to worsen. The new TAM uncertainty also gives a fair indication of what occurs in roll (fig 4b), especially as the batch size, and consequently the number of measurements, increases. Using the adjusted uncertainty in this manner actually creates an upper bound to the attitude uncertainty, and as the batch size increases, the bound converges upon the actual attitude accuracy. Figure 4b shows that the roll uncertainty is converging to 0.28 degrees which then implies that the minimum attitude uncertainty in roll is 0.28 degrees (one sigma). Comparing this to the pitch and roll results show that the roll uncertainty is by far the dominant component of the overall attitude uncertainty.

#### Case 2 : Variation of Attitude Uncertainty with Time of Year

Each of the pitch, roll, and yaw solutions gets better as the batch size increases (from single frame up to a full orbit of data containing nearly 100 measurements). Figure 5 shows the uncertainties versus different times of the year for a variety of batch sizes. These plots use, for the batch start time, the ascending node. Each batch on these plots start at 60 seconds from ascending node; other starting positions in the orbit display similar results.

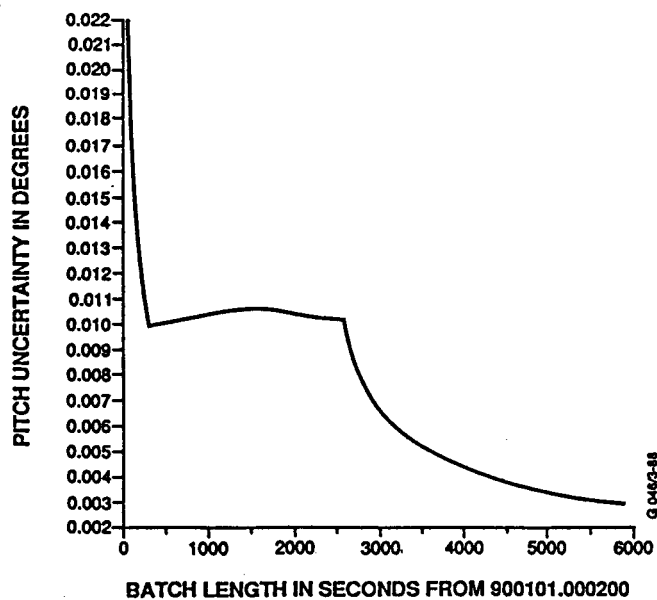
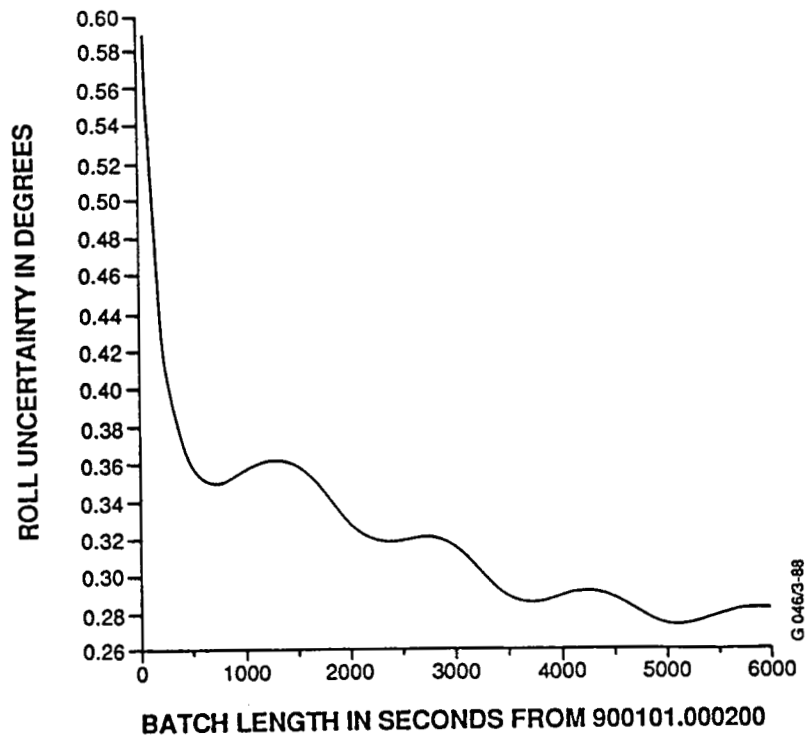
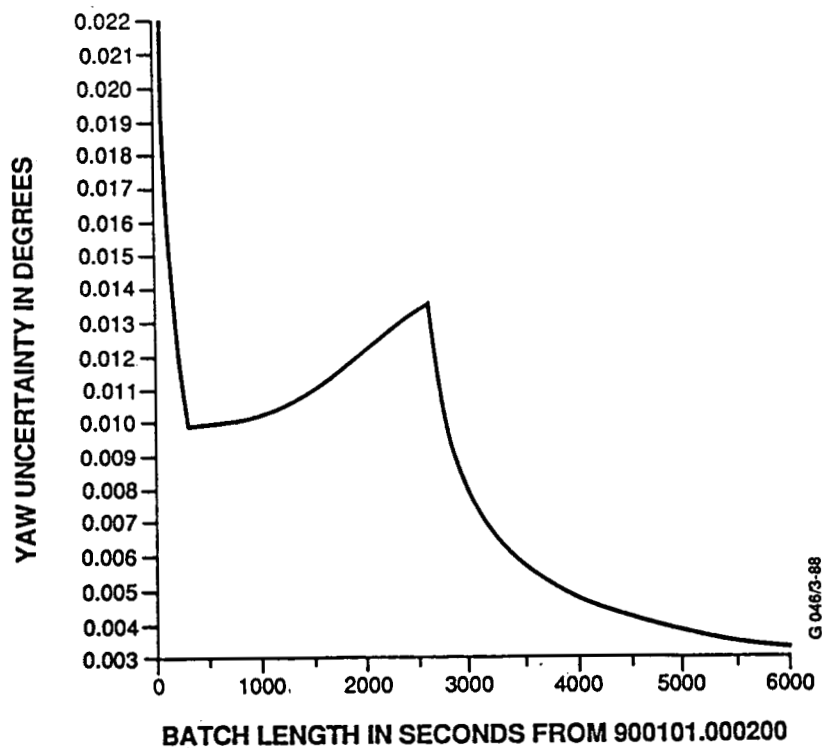


FIGURE 4a  
PITCH UNCERTAINTY vs BATCH LENGTH



**FIGURE 4b**  
**ROLL UNCERTAINTY vs BATCH LENGTH**



**FIGURE 4c**  
**YAW UNCERTAINTY vs BATCH LENGTH**

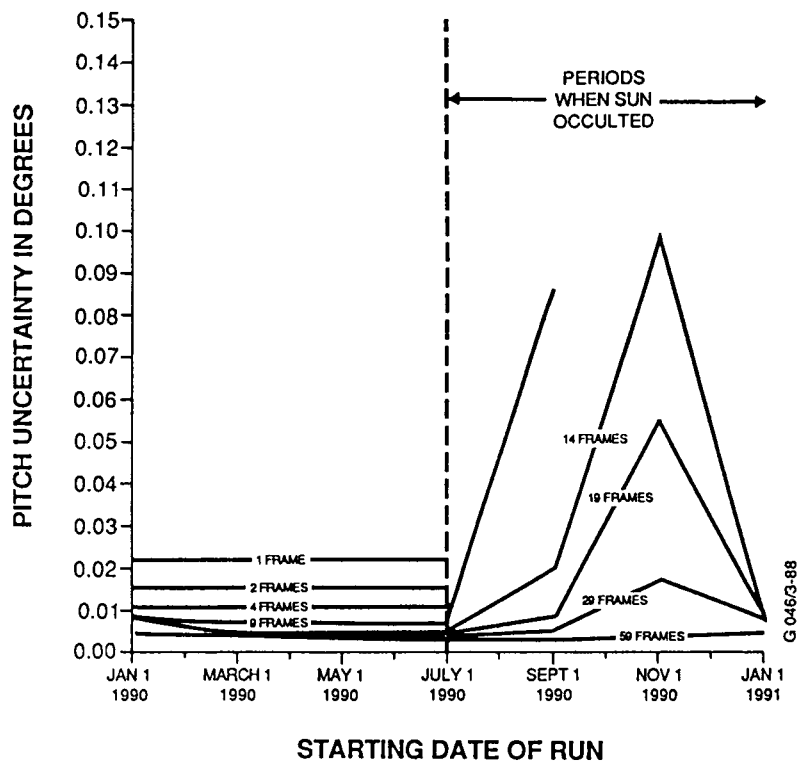


**FIGURE 5a**  
**PITCH UNCERTAINTY vs SUN POSITION**  
**FRAMES - 61 SECONDS APART**

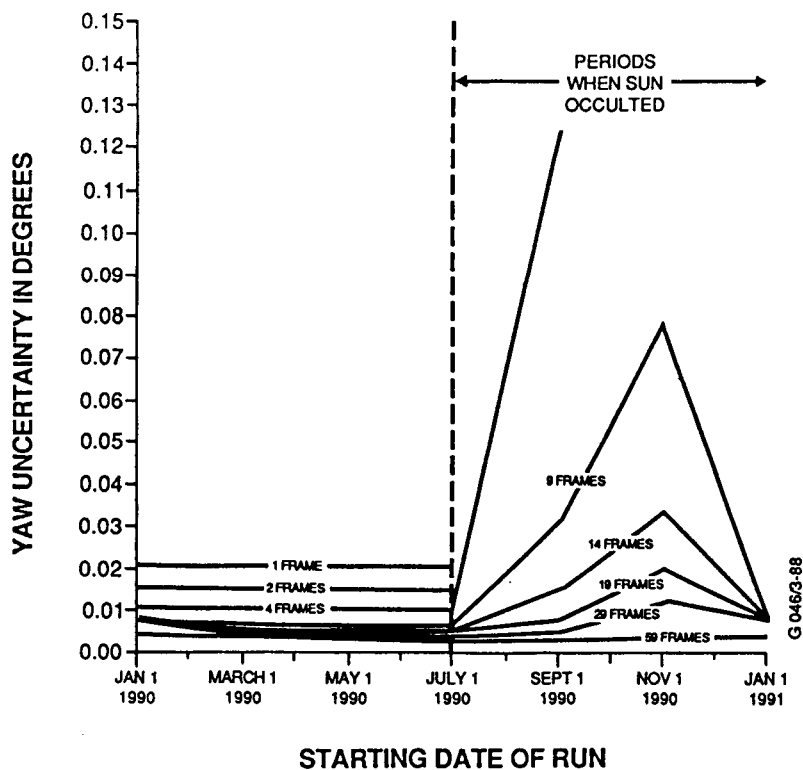


**FIGURE 5b**  
**YAW UNCERTAINTY vs SUN POSITION**  
**FRAMES - 61 SECONDS APART**

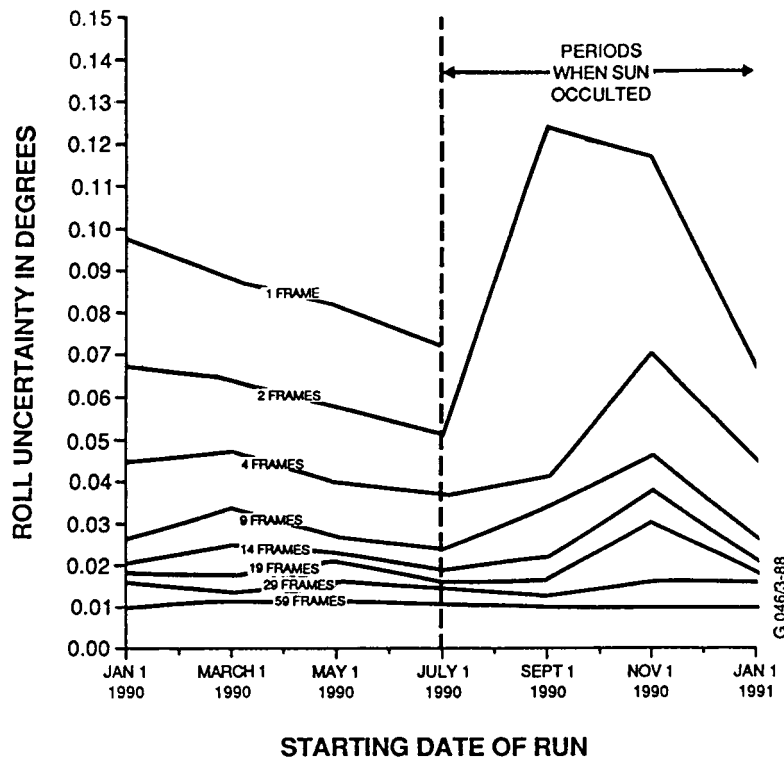


**FIGURE 5c**  
**ROLL UNCERTAINTY vs SUN POSITION**  
**FRAMES - 61 SECONDS APART**

In each of pitch, roll, and yaw the single frame solution is accurate to better than 0.1 degrees assuming that the Sun sensors receive data. In fact, pitch and yaw can be determined to 0.022 (the accuracy of the Sun sensors) single frame. After only two measurements, roll can be determined roughly as well without Sun as the single frame with Sun. Roll can be determined with Sun better than 0.07 degrees. Two frames in pitch and yaw yield 0.015 degrees uncertainty. The accuracy steadily increases in each direction to better than 0.01 degrees after 60 frames (or roughly an hour or 2/3 of an orbit in this case) with or without Sun coverage.

Again, however, the systematic errors that the magnetometer encounter need to be considered. By including the error in the uncertainty (to correct the weighting) as in Case 1, the results become more realistic. Because of the low weighting of the TAM information the pitch and yaw results remain virtually the same as without the systematic errors except in the smaller batches when there is no Sun coverage and the attitude error is exceptionally poor. The results improve as the batch size increases and Sun data is available in every batch - batches bigger than 30 minutes. However, the systematic error contributes several things to roll results. The results shift upward to give an initial uncertainty for the single frame

solution of roughly 0.5 degrees. The error decreases slightly as the batch size increases, but not as significantly as when not considering the systematic error. One last impact of this new error on roll results is that it effectively puts a floor on the accuracy of 0.28 degrees, just as seen in case one.

### Case 3 : Variation of Single Frame Attitude Uncertainty with Orbit Position

The single frame pitch and yaw uncertainties changed very little through the course of an orbit (except when there is earth occultation of the Sun and the uncertainty becomes infinite) and the course of the year. The pitch and yaw show 0.022 degrees uncertainty consistently, dependent only on the Sun sensor uncertainty.

However, the roll uncertainty (fig 6) varies with changes in the Sun and spacecraft position, and consequently the change in the angle between the Sun vector and the magnetic field vector. These results show that roll can be determined to 0.13 degrees at worst and about 0.055 degrees at best. When including the systematic error in the TAM, the results behave similarly but indicate larger uncertainties. The uncertainties are scaled upward, with the best results approximately 0.3 degrees and the worst roughly 0.4 degrees.

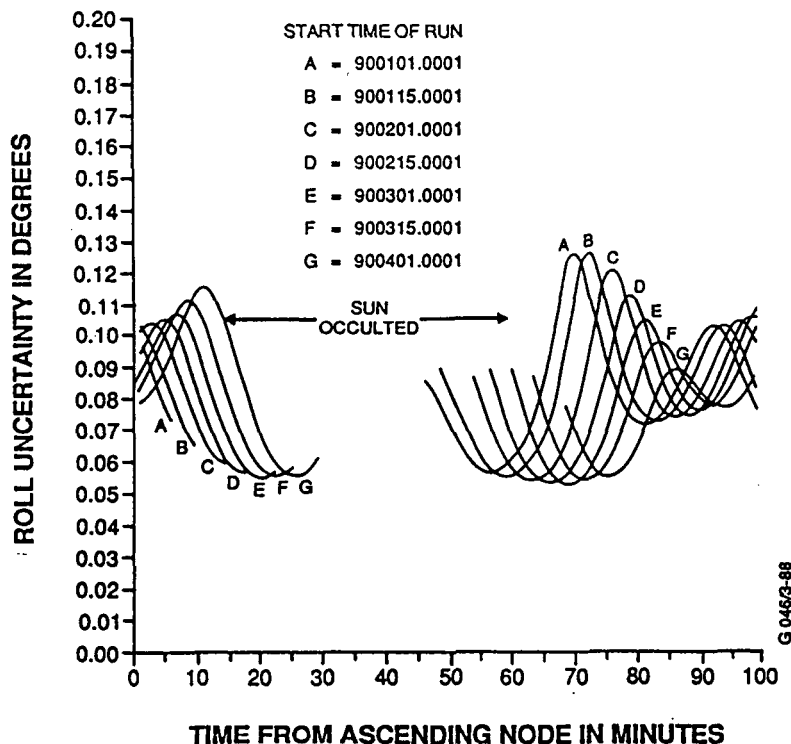


FIGURE 6  
ROLL UNCERTAINTY vs SUN POSITION -  
SINGLE-FRAME SOLUTION

#### Case 4 : Effect of Alignment Uncertainty

Combinations of several of the previous cases became benchmark runs to consider the effect of alignment uncertainty. Variation from previous cases was on the order of  $10^2$  degrees, roughly the order of the specification for the sensor three sigma misalignments. In general, this additional uncertainty is not of great concern.

#### 2.2: Deterministic Attitude Estimate Study

For this contingency scenario using only a single FSS and a TAM, it is assumed that the GRO spacecraft is in Sun pointing mode. In configuring a TRIAD analysis, the FSS boresight, which GCS requires to be the X-axis (see appendix .), therefore points almost directly at the Sun. Using this information, the general case of the FSS/TAM can be configured in two unit vectors (ref 7):

$$\hat{W}_1 = (1, 0, 0)^T \quad \hat{W}_2 = (M_x, M_y, M_z)^T$$

Where  $\hat{W}_1$  = the Sun unit vector observed from the Sun sensor  
 $\hat{W}_2$  = the magnetic field vector observed from the TAM

The TRIAD algorithm is a deterministic method for computing the attitude from two vector measurements (ref 2). Using the TRIAD algorithm, it can be shown that the x,y,z (roll, pitch, yaw) attitude covariance is:

$$P = \sigma_1^2 I + (1/\sin \gamma) [ (\sigma_2^2 - \sigma_1^2) \begin{bmatrix} 1 & 0 & 0 \\ 0 & 0 & 0 \\ 0 & 0 & 0 \end{bmatrix} + \sigma_1^2 \cos \gamma ( \begin{bmatrix} 1 \\ 0 \\ 0 \end{bmatrix} \hat{W}_2^T + \hat{W}_2 \begin{bmatrix} 1 & 0 & 0 \end{bmatrix} ) ]$$

$$= \begin{bmatrix} \sigma_1^2 + (1/\sin^2 \gamma) (\sigma_2^2 - \sigma_1^2 + 2\sigma_1^2 \cos^2 \gamma) & \sigma_1^2 \tan \gamma \cos \psi & \sigma_1^2 \frac{\tan \gamma}{\sin \psi} \\ \sigma_1^2 \tan \gamma \cos \psi & \sigma_1^2 & 0 \\ \sigma_1^2 \tan \gamma \sin \psi & 0 & \sigma_1^2 \end{bmatrix}$$

where:  $\gamma$  = the angle between  $\hat{W}_1$  and  $\hat{W}_2$   
 $\psi = 90 \text{ degrees} - \gamma$   
 $\sigma_1$  = the Sun sensor measurement uncertainty  
 $\sigma_2$  = the TAM measurement uncertainty

From P, roll is the only direction that gamma effects, and only  $\sigma_1$  contributes to pitch and yaw. The single frame GCS results confirm this.

Case 3 shows how the single frame solution changes around an orbit. Figure 6 displays the change in roll, the only direction affected by the changing gamma. Assuming the magnetic field model is roughly a dipole, the roll accuracy should not change much over the course of the GRO's low 28.5 degrees orbit. The GCS results, varying only 0.1 degrees around the

orbit, confirm this. However, clear variations can be seen in the GCS results. Choosing the same position in orbit, different times of year yield different uncertainties. At 65 seconds from ascending node (roughly 2/3 of an orbit) for example, on January 1 in that position the uncertainty is high and on March 1 it is relatively low. The TRIAD result confirms this: Figure 7 shows that  $\gamma$  is larger on March 1 than on January 1, and the formula for  $P$  indicates that this will yield a smaller roll uncertainty.

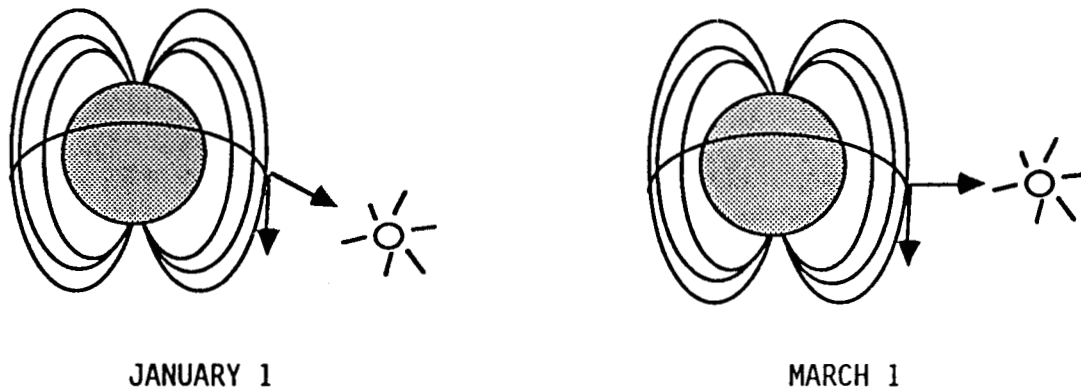


FIGURE 7

### 3.2: Coarse Sun Sensor/Magnetometer Configuration

#### Spacecraft and Sensor Assumptions

Benchmark cases were run for a coarse Sun sensor and magnetometer scenario paralleling the FSS/TAM study (section 3.1). The GRO CSS's are all in the same plane, and in Sun pointing mode this plane is perpendicular to the spacecraft X axis. The four CSS measurements are combined in pairs to produce two angular Sun measurements relative to an effective boresight along the X axis. This may be modeled using a single GCS Sun sensor model aligned with the boresight along the X axis :

CSS : (0,0,0)

The effective uncertainty for the GCS model is then set to 0.707 (see appendix) times the actual analog CSS uncertainty. The actual CSS uncertainty is 0.33 degrees (one sigma). The results for each of the cases run for FSS/TAM scenario turned out to follow the results of the cases involving the FSS/TAM. Each case gave similar results qualitatively to the FSS scenario. The GRO CSS is much less accurate than the GRO FSS which results in a consistently less accurate solution.

When only considering the random error in the magnetometer model, the attitude solution is as good as 0.1 degrees in pitch and yaw and 0.25 degrees in roll after more than 20 frames of data. When including the systematic error, as in the case of the FSS, the pitch and yaw results remain unchanged. However, roll can only be determined to between 0.6 and

0.7 degrees single frame and never better than 0.5 degrees as the batch size increases (one sigma).

The similarities in the results between the FSS and the CSS case are reasonable in that they both represent one (effective) sun sensor measurement, intuitively they should only differ by a scale factor.

### III: Attitude Determination Using Star Trackers

#### 3.1: Star Tracker/Sun Sensor Configuration

For completeness and comparison purposes, this study also includes normal operation scenarios. During normal operations, the GRO is inertially pointing. A specific position in orbit, time of year, and proper FSS and FHST were selected to provide sufficient sensor coverage. The FHST was aligned and its measurement uncertainty set according to spacecraft and sensor specifications.

Results of benchmark runs (similar to those made for the contingency cases) show that GCS predicts that the spacecraft will be able to meet ground attitude requirements. Assuming some sensor coverage, an accuracy of better than 0.005 degrees one sigma can be achieved in each direction with only two or three frames of results. The three sigma requirement is 167.5 arcsec per axis which converts to roughly 0.047 degrees; the one sigma results obtained show that the attitude can be determined to 0.015 degrees three sigma with only a few measurements - well within the requirement.

The TRIAD calculations employed in the FSS/TAM scenario can be examined in a similar fashion for the FSS/FHST case. Because the spacecraft is no longer Sun pointing, the TRIAD set up must be adjusted. However the spacecraft can be simply assumed to be star pointing instead of Sun pointing. Because the FHST is the more accurate of the two sensors, it should be the first of the two vectors ( $\hat{W}_1$  in section 2.2). So again, only roll will be effected by the uncertainty of both sensors, where pitch and yaw will be determined only by the FHST. The angle separating the two measurement vectors is small at roughly 135 degrees because of the relative alignment of the sensors and their fields of view. This checks out in the GCS results in that pitch and yaw show similar results where roll appears slightly worse.

#### 3.2: Two Star Tracker Configuration

Using a setup for two FHSTs as prescribed by sensor and spacecraft specifications, benchmark cases were again examined similar to the study done for the FSS/FHST scenario. Sensor coverage is not so much a factor (except for Earth occultation) so virtually any attitude and time suffices for the study.

Results of the benchmark runs again show favorable results. Single frame solutions are as good as 0.055 in pitch and roll and 0.0035 in yaw. After roughly five frames of measurements, pitch and roll are known to 0.025

degrees and yaw to 0.002 degrees one sigma. After a short period of receiving data in both sensors, attitude can be determined to better than 0.005 degrees in pitch and roll and 0.001 in yaw. These latter results - assuming a small amount (one/two frames) of data in both sensors - compare well with the requirement. The three sigma requirement for two FHSTs is 86.4 arcsec per axis. Converting the GCS results, when there is data from at least one sensor, attitude can be determined to at best 54 arcsec per axis (yaw can be determined to 11 arcsec) three sigma.

#### IV: Conclusions

The GCS study for the contingency FSS/TAM scenario investigated in this paper shows that pitch and yaw can be determined quite accurately without the use of FHSTs. The three sigma result in these directions is 0.066 degrees for a single frame solution. Increasing the batch size does improve the solution, when the Sun is visible to the Sun sensors. Over a large batch of 60 frames (measurements a minute apart) or more, the three sigma pitch and yaw uncertainty improves to better than 0.009 degrees. Including geometric considerations does not alter the pitch and yaw results. As long as the Sun sensor is receiving data and/or the batch spans the eclipse, these results are valid for any time of the year or position in orbit. Although small misalignment uncertainties do not affect the results significantly, a more detailed study with larger variations outside the GRO specification could be useful.

Roll cannot be determined as well as pitch and yaw using FSS/TAM in Sun pointing mode, it can still be determined to a reasonable uncertainty. Again, geometric considerations did not change results dramatically; section 2 notes subtle changes through position in orbit and time of year. With careful handling of systematic TAM errors, a single frame solution yields a three sigma uncertainty of approximately 1 degree. Over a large batch, the three sigma uncertainty approaches 0.75 degree.

The results for CSS/TAM parallel the FSS/TAM scenario while having consistently higher uncertainty in each direction. When examining a batch of 20 frames or more, the three sigma pitch and yaw uncertainty is 0.3 degrees. In roll, the three sigma uncertainty including only random errors is 0.75 degrees. Including systematic errors, the roll single frame solution can only be determined to between 1.8 and 2.1 degrees three sigma. Over a large batch, the three sigma uncertainty in roll including systematic errors remains over 1.5 degrees.

Overall, The GRO attitude can be determined to roughly 0.75 degrees (three sigma) using FSS/TAM and to 1.5 degrees (three sigma) using CSS/TAM. It has been shown that virtually all of this error is in roll; the direction of the X axis can therefore be determined quite well but the roll rotation about this axis is difficult to determine.

GCS proved to be an excellent software tool to examine the GRO ground attitude error. GCS provided the flexibility to perform several different parametric studies. GCS also generated a large quantity of

numerical results necessary for attitude error analysis. With the addition of simple hand calculations, GCS results furnished insight into the existence and growth of attitude errors.

## Appendix

This appendix examines the mathematics used in GCS, including overview descriptions of the filter GCS assumes and the covariance analysis it employs. This section also describes the GCS consider parameter and its uses. GCS spacecraft sensor modeling is discussed as well. This section addresses how the Attitude Ground Support System determines attitude operationally is addressed in light of the GCS system.

### A.1 Batch Least Squares Filter, Loss Function, State Estimate, and Covariance Analysis

The methods used in GCS to calculate attitude determination errors are much like those used to determine attitude near real time for GRO operationally. Both systems assume a batch least squares filter, and results can therefore be readily compared; even though the real time attitude determination system uses a different method (QUEST), results can still be compared qualitatively to GCS output. Although GCS does not actually model the filter that the fine attitude determination system does- a batch least squares filter (GCS does not use a filter at all, it never actually estimates the state parameters using real data) - the manner in which the GCS covariance analysis predicts the attitude accuracy does involve using selected observations from a batch least squares filter. So in order to clearly describe the covariance analysis performed in GCS, a brief discussion of the batch least squares filter is useful.

In general, the batch least squares filter, in computing the state vector value that best fits some data, works to minimize the residual error in the attitude estimate. Simply put, minimizing the weighted sum of the squares (of the components) of the residual error results in the best fit. The resulting loss function (to be minimized) is therefore:

$$J = 1/2 [\vec{y} - \vec{y}_c]^T W [\vec{y} - \vec{y}_c] \quad (A-1)$$

where :  $\vec{y}$  = real measurements made up of:

$\vec{y}_c = \vec{y}_c(\vec{x}_t) + \vec{v}$   
 $\vec{y}_c$  = computed predicted sensor measurements  
as a function of the true state ( $\vec{x}_t$ )

$\vec{v}$  = random measurement noise

therefore  $[\vec{y} - \vec{y}_c] = \Delta \vec{y}$  = residual error  
 $W$  = weighting matrix

The weighting matrix used in GCS is the inverse of the measurement covariance matrix,  $M$ , which is a diagonal matrix whose diagonal elements are the expected standard deviation in the uncertainty of its corresponding measurement. So an observation with a high uncertainty gets little weight.

It is important to note that since M is a diagonal matrix, with zeros off the diagonal, GCS assumes there is no correlation between the observations. Assuming that the observations have a gaussian noise distribution and since these observations are weighted by W, the inverse of the measurement covariance matrix, this least squares fit turns out to be the Maximum Likelihood Estimate (MLE).

Lastly, GCS includes, in its filter model, some a priori knowledge of the state vector. This a priori knowledge is expressed in the form of an initial state covariance matrix and is the expectation value of  $[\vec{x}_0 \vec{x}_0^T]$ , where  $\vec{x}_0$  is the a priori estimate:

$$P_0 = E [\vec{x}_0 \vec{x}_0^T] = \begin{bmatrix} u_1^2 & 0 & 0 & \dots & 0 \\ 0 & u_2^2 & 0 & \dots & 0 \\ \vdots & \vdots & \vdots & \ddots & \vdots \\ 0 & \dots & \dots & \dots & u_n^2 \end{bmatrix} \quad (A-2)$$

Each of the diagonal elements in  $P_0$  is the square of the standard deviation - representing the uncertainty in the corresponding state parameter. Again there is no correlation in the initial state uncertainties as seen in the off diagonal zeros. So including this a priori knowledge,  $\vec{x}_0$ , in the loss function to be minimized, it reads:

$$J = 1/2 (\vec{y} - \vec{y}_c)^T W (\vec{y} - \vec{y}_c) + 1/2 (\vec{x} - \vec{x}_0)^T P_0^{-1} (\vec{x} - \vec{x}_0) \quad (A-3)$$

To minimize J, the partial derivatives with respect to each state element are set equal to zero, creating simultaneous equations corresponding to each of the undetermined state vectors:

$$0 = \frac{\partial J}{\partial \vec{x}} = (\vec{x} - \vec{x}_0)^T P_0^{-1} - (\vec{y} - \vec{y}_c)^T W \frac{\partial \vec{y}_c}{\partial \vec{x}} \quad (A-4)$$

These equations are solved iteratively and are made linear about the previous estimate,  $\vec{x}_k$ . Begin with the a priori state estimate:

$$\vec{y}_c = \vec{y}_c(\vec{x}_k) + H(\vec{x} - \vec{x}_k) \quad (A-5)$$

Where: H = matrix of partials evaluated at  $\vec{x}_0$

The new state estimate can therefore, using equation (A-5) in equation (A-4), be expressed as:

$$\vec{x}_{k+1} = \vec{x}_k + (P_0^{-1} + H^T W H)^{-1} (H^T W (\vec{y} - \vec{y}_c(\vec{x}_k)) + P_0^{-1} (\vec{x}_0 - \vec{x}_k)) \quad (A-6)$$

This equation is iterated until convergence is achieved. The expected uncertainty in the estimate can be derived in the following manner. If  $\vec{e}$  is the error representing the difference in the computed state from any given state determination (using real data that contains noise), then the covariance matrix P represents the expected value of  $\vec{e} \vec{e}^T$ . Using equation

(A-6) and making  $\vec{x}$  the new state estimate, the state can be adjusted until convergence is reached:

$$P_0^{-1}(\vec{x} - \vec{x}_0 + (\hat{x} - \vec{x})) = H^T W [\vec{y} - \vec{y}_c(\vec{x}) + H(\vec{x} - \hat{x})] \quad (A-7)$$

where:  $\vec{x}$  = the true state  
 $\hat{x}$  = the converged estimate

Letting  $\vec{v}$  be the resulting noise in the measurements,  $\vec{e} = \vec{x} - \hat{x}$  be the difference between the true state and the converged estimate, and using equation (A-7), it can be shown that:

$$P = E(\vec{e}\vec{e}^T) = (P_0^{-1} + H^T W H)^{-1} \quad (A-8)$$

GCS uses this covariance equation. The final state uncertainty results that come from GCS are the standard deviations acquired by taking the square roots of the diagonal elements of the final covariance matrix.

## A.2 Consider Parameters

GCS gives the user the ability to incorporate parameters that are not necessarily estimated (or "solved for"), yet whose uncertainties could still effect state uncertainties (in addition to any measurement noise effect), hence the name "consider parameter." Any parameter that GCS employs as a possible state parameter can instead be used as a consider parameter.

Let  $\vec{x}_c$  represent the consider parameters. Also let  $H_c$  be the matrix containing the partials of the measurements with respect to the consider parameter. The effect of the consider parameter error,  $\vec{e}_c$ , on a first order estimate of the state measurement error can be shown :

$$d\vec{y}_c = H_c \vec{e}_c \quad (A-9)$$

Then by adding the effect of the consider parameter to the effect of the noise the adjusted state (which is being solved for) can be computed:

$$\vec{e} = (P_0^{-1} + H^T W H)^{-1} (P_0^{-1} \vec{e}_0 - H^T W H_c \vec{e}_c + H^T W \vec{v}) \quad (A-10)$$

where:  $\vec{e}_0$  = a priori state error  
 $\vec{v}$  = noise

Taking the expected value of the product of  $\vec{e}\vec{e}^T$ , it can be shown that :

$$P = E[\vec{e}\vec{e}^T] = P_s + P_s Q_c P_c Q_c^T P_s \quad (A-11)$$

where:  $P_s = (P_0 + H^T W H)^{-1}$  for compactness  
 $Q_c = H^T W H_c$  for compactness  
 $P_c = E[\vec{e}_c \vec{e}_c^T]$  = the consider parameter covariance matrix,  
a diagonal matrix with the diagonal elements  
representing the expected uncertainty in the  
corresponding consider parameter

$P_{SQ} P_{QC}^T P_{SC}$  therefore represents the consider parameter contribution to the covariance. It is this equation (A-11) that GCS uses to calculate the state covariance assuming the existence of consider parameter effects. It should also be noted that the contribution from each of the consider parameters is independent (since the covariance matrix in (A-11) is diagonal), and that GCS computes the separate as well as the total contribution.

### A.3 Sensor Modeling in GCS- GRO Specific

This subsection describes how GCS models the sensors on the GRO, including the Fixed Head Star Tracker (FHST), the Fine Sun Sensor (FSS), the Coarse Sun Sensor (CSS), and the Three Axis Magnetometer (TAM). GCS models other sensors (including those for spinning spacecraft) whose models are not considered here. For the partial derivatives pertaining to these sensor models in GCS, see appendix I of reference 1.

#### A.3.1 Fixed Head Star Trackers

GCS models two FHST's either simultaneously or separately (and/or in conjunction with other sensor(s)). GCS defines the FHST coordinate system such that  $X_S$  is along the sensor boresight,  $Y_S$  is along the direction of the +V measurement, and  $Z_S$  is positioned so that  $X_S, Y_S, Z_S$  form a right handed coordinate system. The horizontal and vertical coordinates of the star locations in the FHST field of view,  $Y_H$  and  $Y_V$  respectively, are defined in GCS:

$$y_H = (1/S_H) (H + b_H) \quad (A-12)$$

$$y_V = (1/S_V) (-V + b_V) \quad (A-13)$$

$$\text{where : } H = \tan^{-1}[F_{SZ}/F_{SX}] \quad (A-14)$$

$$V = -\tan^{-1}[F_{SY}/F_{SX}] \quad (A-15)$$

$(F_{SX}, F_{SY}, F_{SZ}) = F_S$ , the unit star vector in the FHST sensor coordinate system.

The angle H rotates from the  $\hat{Y}_S - \hat{F}$  plane to the  $\hat{Y}_S - \hat{X}_S$  plane about the  $\hat{Y}_S$  axis. The V angle rotates from the  $\hat{Z}_S - \hat{F}$  plane to the  $\hat{Z}_S - \hat{X}_S$  plane about  $\hat{Z}_S$ . The state parameters are:

$$y_H = y_H(p, r, y, \phi_1, \phi_2, \phi_3, S_H, b_H) \quad (A-16)$$

$$y_V = y_V(p, r, y, \phi_1, \phi_2, \phi_3, S_V, b_V) \quad (A-17)$$

where p, r, y = pitch, roll, and yaw

$\phi_1, \phi_2, \phi_3$  = sensor alignment parameters

$S_H, S_V$  = sensor scale factors

$b_H, b_V$  = sensor biases

#### A.4.2 Fine Sun Sensor

Although GCS has a Fine Sun Sensor model, the GCS Coarse Sun Sensor more

closely models the GRO FSS uncertainties in that the GCS CSS is a digital sensor like GRO's FSS and the GCS CSS presents the simpler model (which is sufficient to model GRO's FSS). GCS can model up to three CSS's simultaneously; when modeling GRO, only two are necessary. The sensor detects the Sun's direction (expressed as a unit vector in CSS coordinates, which can be transformed to the unit Sun vector,  $S_I$  in GCI coordinates):

$$\hat{S}_S = (S_{SX}, S_{SY}, S_{SZ}) \quad (A-18)$$

$$= [M][B][A] S_I \quad (A-19)$$

where:  $[M]$ ,  $[B]$ ,  $[A]$  = matrix coordinate transforms

in terms of an  $\alpha$  angle and a  $\beta$  angle (fig 8). GCS corrects these measurements using calibration coefficients,  $A_1, A_2, B_1, B_2$ :

$$N_\alpha = 1/A_2 (\alpha - A_1) \quad (A-19)$$

$$N_\beta = 1/B_2 (\beta - B_1) \quad (A-20)$$

and

$$\alpha = \tan^{-1}(S_{SY}/S_{SX}) \quad (A-21)$$

$$\beta = \tan^{-1}(S_{SZ}/S_{SX}) \quad (A-22)$$

This GCS model assumes that the CSS boresight is along the  $X_S$ -axis,  $\alpha$  is the projected sun angle in the  $X_S$ - $Y_S$  plane, and  $\beta$  is the projected sun angle in the  $X_S$ - $Z_S$  plane. The state parameters for the GCS CSS are:

$$N_\alpha = N_\alpha(p, r, y, \phi_1, \phi_2, \phi_3, A_1, A_2) \quad (A-23)$$

$$N_\beta = N_\beta(p, r, y, \phi_1, \phi_2, \phi_3, B_1, B_2) \quad (A-24)$$

where :  $p, r, y$  = attitude parameters that define  $[B]$   
 $\phi_1, \phi_2, \phi_3$  = CSS alignment parameters (defining  $[M]$ )  
 $A_1, B_1, A_2, B_2$  = sensor calibration parameters

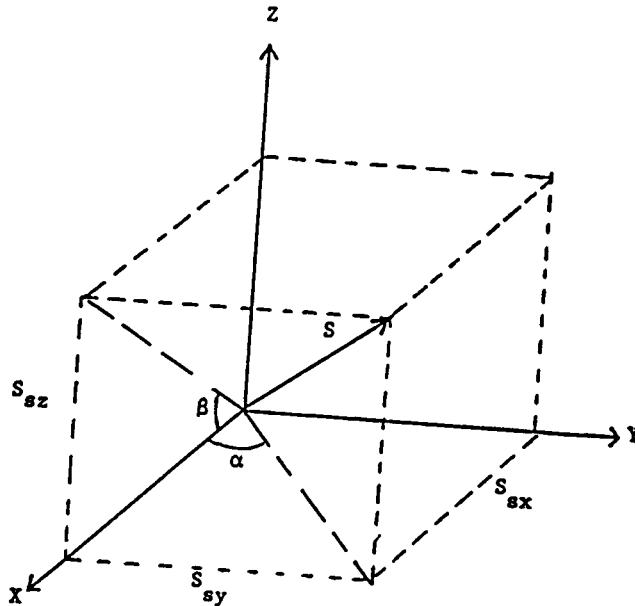


FIGURE 8. DIRECTION OF SUN VECTOR IN CBS

#### A.4.3 Coarse Sun Sensor

GRO's CSS is an analog sensor which is not modeled by GCS. However, a scale factor was determined so that the GCS CSS model, described in A.4.2, could be used. It can be shown that:

$$\sigma_2 = \sqrt{2} / 2 \sigma_1 \quad (A-25)$$

where  $\sigma_1$  = uncertainty for the GRO CSS  
 $\sigma_2$  = uncertainty for the GCS CSS

#### A.4.4 Three Axis Magnetometer

In GCS the TAM measurement vector in the sensor frame is in the direction of the geomagnetic vector:

$$\vec{Y} = [M][B][A]\vec{H}_I + \vec{b} \quad (A-25a)$$

$$= [M][B]\vec{H}_R + \vec{b} \quad (A-25b)$$

where  $[M], [B], [A]$  = transformation matrices (see ref 1, 3.3)  
 $\vec{H}_I$  = geomagnetic field in GCI coordinates  
 $\vec{H}_R$  = " " reference coordinates  
 $\vec{b}$  = bias

GCS uses the magnetic field model from the subroutine MAGFLD (ref 5). The state parameters for the GCS TAM are:

$$Y = Y(p, r, y, \phi_1, \phi_2, \phi_3, \vec{b}) \quad (A-26)$$

where:  $p, r, y$  = attitude parameters defining  $[B]$   
 $\phi_1, \phi_2, \phi_3$  = alignment parameters defining  $[M]$   
 $\vec{b}$  = constant bias vector

#### Acknowledgement

The author would like to thank Mr. E. Seidewitz and Dr. F. L. Markley of MASA Goddard Space Flight Center for their help, guidance, and insight.

#### References

1. Blaisdell, Bilanow, Chen, Talukdar, and Seidewitz "Generalized Calibration System (GCS) Version 2.3 User's Guide," General Sciences Corporation, GSC-TR8713, April, 1987.
2. Shuster, M.D. and Oh, S.D. "Three Axis Attitude Determination from Vector Observations," Journal of Guidance, Control, and Dynamics, Vol. 4, No. 1, Jan/Feb 1981, pp 70-77.
3. Tracewell, D., Ketchum, E., Harman, R., "GRO Mission, Flight Dynamics Analysis Report: Review of Sensor Characteristics (Analysis Item A3.3)," May, 1988.

4. TRW, "Gamma Ray Observatory Mission Contract Critical Design Audit Package Volume II," 40420-85-231-008.

5. Wertz, J. R., Spacecraft Attitude Determination and Control. Dordrecht: D. Reidel Publishing Company, 1978.